Experimental Investigation of Aerodynamic Characteristics of NACA 23015 under different angles of attack and Comparison with Available Package

Mohammed Ahmed Rasheed* & Ahmed Adnan AL-Qaisy*

Received on: 5/5/2008
Accepted on: 7/8/2008

Abstract

A Model of wing section of type (NACA 23015) had been built to be investigated and study the aerodynamic characteristics in a subsonic wind tunnel at different angles of attack in order to calculate the aerodynamic coefficients such as lift, drag, moment and pressure coefficients. The effect of changing the angle of attack on the aerodynamic coefficients was investigated. Then a virtual model of the wing section and wind tunnel had been programmed and tested by available standard packages such as the (Design Foil) Program which uses Panel Method to calculate the aerodynamic coefficients, and the finite element package (Ansys Ver.9). A comparison was made to the arrived results with the experimental data to check the accuracy of the results, and both experimental and theoretical results were convergent. The percentage of similarity between the experimental and theoretical was 83% for the Aerodynamic characteristics.

بحث عملي حول الخواص الديناهوائية لمقطع جنح مطيار نوع " NACA 23015 " لزوايا طيران مختلفة مع مقارنة النتائج بالتطبيقات الجاهزة

الخلاصـــة

تم في هذا البحث تصنيع مقطع مطيار من النوع (NACA 23015) واختباره داخل نفق هوائي تحت صوتي ولزوايا هجوم مختلفة لغرض دراسة الخواص الديناهوائية له.ومن ثم حساب المعاملات الديناهوائية كمعامل الرفع ، معامل الكبح ، معامل العزم ومعامل الضغط .كما تم دراسة تأثير زوايا الهجوم المختلفة على تلك المعاملات .تم بناء نموذج حاسوبي للمقطع والمجرى الهوائي ونفذ ببرنامج (Design Foil) والذي يستعمل طريقة الأسطح المحددة (Panel Method) في إيجاد المعاملات الديناهوائية وكذلك تم بناء نموذج افتراضي أخر مصمم ببرنامج (Ansys Ver.9) وذلك لمقارنة النتائج العملية المستخلصة مع النتائج التي تم الحصول عليها من هذين البرنامجين لمعرفة مدى تطابق النتائج العملية مع النتائج النظرية ،والقرار على أفضلية البرامجيات الجاهزة من عدمه. وكان التطابق بنسبة 83% مع النتائج العملية بالنسبة للخواص الديناهوائية.

Nomenclature

AR	Aspect ratio	-	
b	Span	mm	
c/a	Mid thickness to radius ratio(thickness ratio)	-	
C	The Chord of the Airfoil	mm	
C_D	Drag coefficient	-	
C_L	Lift coefficient	-	
C_m	Moment coefficient	-	
C_{mx}	Pitching Moment Coeff. in x – Direction	-	
C_{mz}	Pitching Moment Coef. in z – Direction	-	
C_p	Pressure coefficient	-	
C_x	Drag Coef. in x- Direction	-	
C_z	Lift Coef. in z- Direction	-	
D	Drag	N	
H	Local Pressure (heights of Water column)	mm	
h_u	Pressure on the upper section surface	mm	
h_L	Pressure on the lower section surface	mm	
L	Lift	N	
M	Moment on airfoil	N.m	
P	Pressure on airfoil	N/m^2	

***Mechanical Engineering Department, University of Technology/Baghdad**

https://doi.org/10.30684/etj.27.2.1
2412-0758/University of Technology-Iraq, Baghdad, Iraq

P_o	Local Pressure on Wing	N/m^2
P_∞	Freestream Pressure	N/m^2
q_∞	Dynamic Pressure	N/m^2
Re_x	Reynolds Number	-
S	Airfoil surface section area	mm^2
t	Thickness	mm
v	Stream Velocity	m/s
W.T	Wind Tunnel	-
Z_1	Thickness from the Lower Surface of the Wing	mm
Z_2	Thickness from the Upper Surface of the Wing	mm
a	Angle of attack	degree
r_a	Air density	kg/m^3
r_w	Water density	kg/m^3
r_∞	Free stream density	kg/m^3
g	Angle Between C_z & C_x	degree
$\in$	Angle of Slop Tangent	degree

Other subscriptions were defined locally in the text.

Introduction

The investigation of aerodynamic characteristics of different types of airfoil model section is one of the most important fields in aeronautical engineering, to make these investigations there are two ways:

a. Experimental method.

b. Theoretical method.

The experimental method is to investigate the airfoil section model in wind tunnel and then calculate the results to find the aerodynamic coefficients, while the theoretical method is done by using one or more of modeling analyzing software programs though designing the airfoil section model and analyze it in that program .Barely the experimental method is much confidant than the theoretical way in the end if the tests environment was perfect [1]. The purpose of this research is to investigate and calculate the aerodynamic coefficients such as lift, drag, moment and pressure coefficients. The effect of changing the angle of attack on the aerodynamic coefficients was investigated.

Theory

To investigate and calculate lift, drag and pitching moment coefficients from the pressure distribution on the airfoil section model NACA 23015 in the wind tunnel. Figure.(1) represents a section of an airfoil on incidence a to the fluid stream, which is assumed to be from left to right at a speed of (v). Through the nose of the airfoil are drawn axes (ox) and (oz) parallel and perpendicular to the chord line respectively. The chord of the airfoil is denoted by (c). The ordinates of the highest and lowest points of the section are (z_2) and (z_1) respectively, Fig.(2).

The airfoil may or may not be solid in either case its surface is regarded as a thin sheet of material, perfectly rigid with the pressure inside uniform at (P_o), the static pressure of the undisturbed stream this is permissible, since the pressure are to be integrated round the surface and the integral of a uniform pressure over a closed surface is zero. Whatever its magnitude .Taking a slice of the airfoil of unit span wise length, consider the forces acting on a small element, of length (d_s), of the surface. The normal force of the element is composed of (Pd_s) in wards, and (Pod_s) out wards force of $(P - Po)d_s$.

This force may be resolved into component (d_z) and (d_x) acting parallel to the (oz) and (ox) axis respectively then:-

$$d_z = -(P - P_o) d_s \cos\in \quad \ldots\ldots(1)$$

Now, from the geometry of the element $d_S \cos \in = d_x$ where

$$d_z = -(P - P_o) d_x \quad \ldots\ldots(2)$$

This is for an element on the upper surface. For an element on the lower surface it becomes

$$S_z = -(P - P_o) S_x \quad \ldots\ldots(2)$$

If this is now integrated with respect to (x) between the limits of x = 0 and x = c, the integration of d_z becomes the total force z, whence

$$Z = \int_0^c -(P - P_o) dx + \int_0^c (P - P_o) dx. \quad (3)$$

Using subscripts (u) and (l) for the upper and lower surface respectively this becomes:

$$Z = \int_0^c [(P - P_o)_u - (P - P_o)_l] dx \ldots(4)$$

This gives the variation of pressure (P) along the chord of the airfoil it is possible to calculate the lift. It can be seen that, although the pressure inside the airfoil section model was assumed to be (P_o). The actual value is quit immaterial in the present context. The next step will reveal why the particular value (P_o) was chosen. Equation (4) is easily put into coefficient. From as follow define C_z by:-

$$C_z = \frac{z}{1/2\ r\ v^2\ S}$$

Considering unit span the area (s) is equal to the chord (c).

$$C_z = \frac{z}{1/2\ r\ v^2\ C}$$

$$= \frac{-1}{1/2\ r\ v^2\ C} \int_0^c [(P - P_o)_u - (P - P_o)_l] dx$$

$$\ldots\ldots\ldots\ldots\ldots\ldots(5)$$

Dividing by $1/2\ r\ v^2$ inside the square bracket, and remembering that $\frac{1}{c}(dx) = d\left(\frac{x}{c}\right)$ Gives

$$C_z = -\int_0^1 (C_{pu} - C_{pl}) d\left(\frac{x}{c}\right) \ldots\ldots (6)$$

Since $\frac{P - P_o}{1/2\ r\ v^2} = C_P$ by definition.

A similar argument may be used to give the following relation $d_x = (P - P_o) d_s \sin\in \ \Rightarrow\ d_s \sin\in = d_z.$ leading finally to

$$C_x = \int_{z_1/c}^{z_2/c} Cp.d\left(\frac{z}{c}\right) \ldots\ldots\ldots\ldots (7)$$

This coefficient is based on the plane area of the airfoil. The pinching moment may also be calculated from the pressure distribution for simplicity it will be found about the origin of the (ox) and (oz) axes.

$$d_z = -[(P - P_o)_u - (P - P_o)_l]\ dx$$

And therefore the contribution to be pitching moment due to this element of z….force is:-

$$d_M = [(P - P_o)_u - (P - P_o)_l]\ x.dx \ldots(8)$$

Where the total pitching moment due to (Z) is:-

$$C_{Mz} = +\int_0^c [Cp_u - Cp_l]\left(\frac{x}{c}\right)\cdot d\left(\frac{x}{c}\right)$$

$$= -\int_0^c \Delta Cp\left(\frac{x}{c}\right)\cdot d\left(\frac{x}{c}\right) \ldots\ldots\ldots\ldots\ldots (9)$$

Since

$$C_M = \frac{M}{1/2\, r\cdot v^2\cdot S.c} = \frac{M}{1/2\, r\cdot v^2\cdot C^2}$$

where S=c in this cases similarly, the contribution to C_M due to the x….force may be obtained as:-

$$C_{Mx} = \int_{z_1/c}^{z_2/c} \Delta Cp\left(\frac{z}{c}\right)\cdot d\left(\frac{z}{c}\right) \ldots\ldots (10)$$

The integration given above are normally performed graphically. The force coefficient (C_x) and (C_z) are parallel and perpendicular to the chord line where as the more usual coefficient (C_L) and (C_D) are referred to the air direction. The conversion from one pair to the other may be performed by reference to Fig. (2), in which C_R, the coefficient of the resultant both of C_x, C_z and of C_L and C_D and therefore from Fig (2) now [2]:-

$$C_L = C_R \cos(g + a)$$

$$= C_R \cos g\cdot\cos a - C_R \sin g\cdot\sin a$$

And

$$C_R \cos g = C_z \quad and \quad C_R \sin g = C_x$$

Where

$$C_L = C_z \cos g - C_x \sin a \quad \ldots(11)$$

Similarly

$$C_D = C_R \sin(g + a)$$

$$= C_z \sin a + C_x \cos a \quad \ldots.(12)$$

Since

$$C_p = \frac{P - P_\infty}{q_\infty} \quad \ldots\ldots\ldots\ldots\ldots(13)$$

Where $q_\infty = \frac{1}{2}\rho_\infty v^2$ Then

$$C_{p_u} = \frac{P_u - P_\infty}{q_\infty} \quad \ldots\ldots\ldots\ldots\ldots(14)$$

Also

$$C_{p_L} = \frac{P_L - P_\infty}{q_\infty} \quad \ldots\ldots\ldots\ldots(15)$$

Where (*P*) represented by (*h*) experimentally.

Subsonic Wind Tunnel

The subsonic wind tunnel used in current research is an open circuit type with a working cross section of (300mm x 300mm) as schematically shown in Fig.(5). Wind speeds of (36m / sec.) are achievable allowing experiments on many aspects of incompressible air flow and subsonic aerodynamics to be performed at satisfactory Reynolds numbers. The tunnel has a smooth contraction fitted with the protective screen. The working section is constructed of clear Perspex with a cross section of (300mm x 300mm) and a length of (600mm), Figs. (6) and (7) represent photo of the wind tunnel and the working section respectively.

Downstream of the working section, a diffuser which leads to an axial flow fan which is driven by a (5.6 kW three phase A.C motor). The flow is controlled by a butterfly valve before exhausted to atmosphere through exhaust duct. The air enters the tunnel through carefully shaped diffuser. The working section giving full visibility of flow field and the model is supported from one side of the wall. At the downstream there is a pitot static tube, Fig. (8) Shows the pitot tube used here with the wind-tunnel working section, thus the pitot tube is fixed through wind tunnel ceiling. The boundary layer thickness

at the end wall of the wind tunnel test section was found by using the well known formulas for laminar and turbulent boundary layer growth respectively are as follows:-

$$d_{lam.} = \frac{4.64\,x}{\sqrt{\mathrm{Re}_x}}$$ (For laminar flow on flat surface) ……(16)

$$d_{turb..} = \frac{0.37}{\sqrt[5]{\mathrm{Re}_x}}$$ (For turbulent flow on flat surface) ……...(17)

The boundary layer change from laminar to turbulent is regarded as sudden change at (Re_x=500000), so that turbulent boundary layer thickness was found to be about (26mm) at the test section exit which is acceptable and does not affect the test section a lot. The turbulence level at the working section was found [3] to be acceptable.

Wind Tunnel Boundary Corrections:-

The condition under which a model is tested in a wind tunnel are not the same as those in free air. The walls on the model thickness and wake are subjected to solid and wake blocking, solid and wake blocking are usually negligible with an open test section since the air stream is then free to expand in a normal manner Alan Pope [4]. Maskell [5] suggests that the total solid and wake-blocking corrections are calculated as follows:-

$$C_t = \frac{1}{2}\frac{Model\ \ frontal\ area}{Test\ \mathrm{sec}tion\ area}$$

And he found that a maximum ratio of model frontal area to test cross-sectional area 7.5% should probably be used, unless errors of several percent can be accepted.

In the present research, the wing section model frontal area to the test cross-sectional area is equal to 0.85%. This means that the blocking errors are relatively small and may be negligible.

Hints for those models who had ratio more than 7.5% the solid-blocking eq.(18) and wake-blocking eq.(19) corrections are calculated respectively as follows[8]:-

$$\varepsilon_{sb} = K_m (mv) / A^{\frac{3}{2}}$$ ……..(18)

Where

K_m : Wing section Shape factor = 0.74 for this model

mv : Model Volume = 0.7.*t.C.b*

A : Test section area = (93025mm^2) for this wind tunnel

$$e_{wb} = \frac{1}{2}.\frac{C}{h_t}C_{dun}$$ ……..(19)

Where

h_t :Heights of wind tunnel test section

C_{dun} : Uncorrected drag coefficient

Then the Overall Correction Coef. is:-

$$\varepsilon = \varepsilon_{wb} + \varepsilon_{sb}$$ ……..(20)

From This equation the Re_x correction is:-

$$\mathrm{Re}_x = \mathrm{Re}_{xun}(1+e)$$ ……..(21)

And the lift coefficient correction is:-

$$C_L = C_{Lun}(1-s-2e)$$ ……...(22)

Where

$$s = \left(\frac{p^2}{48}\right)\left(\frac{C}{ht}\right)^2$$ ……..(23)

Also the drag coef. correction is:-

$$C_d = C_{dun}(1-3e_{sb}-2e_{wb})$$ ….(24)

Finally the angle of attack correction is:-

$$a = a_{un} + \left(57.3\frac{s}{2p}\right)\left(CL_{un} + 4C_{\frac{m1}{4un}}\right) \quad \text{.....(25)}$$

Where the symbol un represents uncorrected reads

The Wing Section Modeling

A model of wood of the (NACA 23015) had been built locally; the model as we know is un-summitry i.e. the upper surface is different from the lower one. The data for this section were taken from NACA's lists of wings section [9],[10]. And its coordinates is as listed as in (Table 1).

The wing section model specification was, the cord (C = 150mm) and thickness ratio of (15%) ,the section length (b = 305mm). Static pressure taps have been made inside the both sections ,these bores were distributed to 10 bores for each section but un-equally on both sections and the bigger numbers distributed at the front of the both sections fig.(3). Inside the taps a stainless steel pressure pipes were fixed with inner diameter of (0.7mm) and outer diameter of (1mm).

Pitot-Static Tube Corrections

In this research we used a standard pitot-static tube with standard elliptical head shape (N.P.L Standard) to measure airspeed inside the wind tunnel .Where it's diameter was (5mm) and (200mm) long .And the corrections for the pitot-static tube was as[6][7]:-

$$\Delta P = (rH_1)_{water}.g$$

$$= P_{total} - P_{static} = \frac{1}{2}.E.r.u_{\infty}^2 \quad \text{.....(26)}$$

$$E = E_o + \omega + \Omega \quad \text{.....(27)}$$

Where

E : Correction factor

E_o: Represent the effect of distance of static pressure inlet (E_o=0.9976)

ω : Viscosity effect and it's equal to zero for fully developed flow

Ω : The effect of the distance from the tube to the wall and it could be taken from the curve in fig.(8)

The Multi Tubes Manometers

A standard multi tubes manometer had been used to measure the pressure Fig. (7), this type of manometers used liquid water because we work in subsonic criteria. The manometer connected with the stainless steel pressure tubes of the wing section model by a rubber snout.

Effects of Changing Angles of Attack

By changing the angle of attack we found its effects on the aerodynamic characteristics coef. for the section NACA 23015. At the beginning the calculation were performed for the range of angle of attack of ($-10^o \sim 20^o$) but we found that the effecting angles for this section lies between (-9^o) and (15^o) angles of attack, so to reduce the data and calculations the results will be presented for this range of. Figures (9,10,11) shows that (C_{pu}) was decreased while (C_{pl}) was increased also the increment in (Cp) for the upper surface were much higher than that for the lower surface due to the positive increment in (a) while in Figs.(12,13) the case was reversed, yet the increments between the upper and lower surface were less than the 1st case ,which gives as an indications that the upper surface of the wing section is more importance than the lower one, i.e. the flow stream variation for the upper surface is much effective on the aerodynamic

characteristics than the lower surface ,and for that reason all or most of the developments on airplane wings to increase or reduce the boundary layer separation were applied on the upper surface of the wing, also we could know why they construct the engines of the airplane on the lower surface of the wings.

Figures (14, 15 and 16) show the aerodynamics coefficients through different angles of attack and for both experimental and theoretical results from the Design Foil program. Anyway the results were convergent and the experimental data is accurate and acceptable.

The results of (Ansys Ver.9) Figures (17 to 22) show the variation of pressure coefficient among the wing section model the figures shows clearly the increment of pressure coefficient on the leading edge of the wing, also they show that the pressure coefficient at the upper surface of the wing was smaller than the lower surface at the positive angles of attack while in the negative angles the case is reverse which is agree with the experimental results of the W.T and shows a great similar in value with that of the Design Foil program and which make as conclude that the experimental result were accurate and acceptable.

Then the whole results were compared with those which had been taken from the program Design Foil and (Ansys.9), the accuracy of the experimental work was high were the difference was limited because the percentage of identification was 83% after comparing the excremental results with the packages one, which give us an indication that the experimental data was acceptable.

Conclusions

From this research we conclude:-

1-The values of (Cp_u, C_L, C_d) is increased with increasing angle of attack.

2-The value of (Cp_L, C_m) is decreased with increasing angle of attack.

3-The critical angle of attack in the positive position for this wing section model (NACA 23015) is (15^o) , Fig. (14) Illustrates that after the angle (15^o) a drop in (C_L) occurs, while the critical angle of attack in the Negative position for this wing section model (NACA 23015) is (9^o).

4-The separation of the boundary layer at both upper and lower surface of the wing section model (NACA 23015) begins with the increasing or decreasing of the angle of attack and its effects at the upper surface are more than the lower one which is why most ways of controlling separation and boundary layer designed at the upper section of the wings and also because of little effect of separated boundary layer at the lower section of the wing, most airplanes put its engines there.

5-The stole area (i.e. the area without any boundary layer and any movement of flaps at these areas do nothings) at the upper surface which illustrated as a red area in Fig. (11) Starting at the angle of attack equal to (15^o) ,while in the lower surface it begins at the angle of (9^o).

6-The Study recommend to investigate the effects of changing of the aerodynamics characteristic due to change in angles of attack on the structure of the wing section model (NACA 23015), also study the performance ,Stability and controllability for this section.

7-Also we recommended investigating the aerodynamic characteristics of this section for transonic speed with angles changing.

References

[1] Royal air force – UK,“ The Principle of Flight ” , Vol. A , Sec.3 , Ch.2,1992

[2] John D. Anderson , JR., “ An Introduction to Flight ” , 5th Edition . McGraw-Hill, 1995

[3] EL. Houghton & NB. Caruthers, “ Aerodynamics for Engineering ” , 4th Edition . John Wiley, 1998.

[4] Alan Pope & John, J. H., “Low Speed Wind Tunnel”, John Wiley & Sonc., New York / London. 2001

[5] Maskel, C. E., “A Theory of Blockage Effects of Buff Bodies and Stalled Wings in A Closed Wind Tunnel”. ARC R & M 3400,1965.

[6] Kadir N. “Modification of Airfoil Aerodynamic Properties by using Internal Aquatic Excitations Technique “,Msc. Theses , Mechanical Department, University of Technology. Iraq, 2005.

[7] Chue S. H., “Pressure Probes For Fluid Measurement”, Progress in Aerospace Sciences,Vol.16, No.2, pp. 147 – 223, 1975.

[8] “ Journal of the Royal Aeronautical Society ” ,Vol.64 , No.596 , P.449-464 , Aug.1960 & Vol.61 , No.553 , P.37-42 , Jan.1957.

[9] I. H. Abbott & A. E. Van Doenhoff , “ Theory of wing Section ” , McGraw-Hill ,NY. 1959.

[10] Alan Pope , “ Basic Wing & Airfoil theory ” , McGraw-Hill . 1951.

[11] L. J. Clancy, “ Aerodynamics ” , 5th Edition .1997.

[12] Charles E. Dole, “ Flight theory and Aerodynamics ” , John Wiley .1981.

[13] John J. Bertin & Michael L. Smith, “ Aerodynamics for Engineering ” , Prentice Hall. 1979.

[14] A. E. Brock & E. L. Houghton, “ Aerodynamics for Engineering and Students ” , McGraw-Hill, London. 1960 .

[15] A. C. Kermode , “ Mechanics of Flight ” , Pitman Publishing /London. 1977.

[16] Charles E. Dole “Flight Theory and Aerodynamic” (John Wiley-1981).

Table (1) The Coordinates of the wing section model NACA23015

Upper Surface		Lower Surface	
X (mm)	Y (mm)	X (mm)	Y (mm)
0	0	0	0
1.875	5.01	1.875	2.31
3.75	6.66	3.75	3.375
7.5	8.835	7.5	4.56
11.25	10.35	11.25	5.415
15	11.46	15	6.135
22.5	12.78	22.5	7.26
30	13.38	30	8.115
37.5	13.62	37.5	8.67
45	13.575	45	8.94
60	12.885	60	8.88
75	11.61	75	8.25
90	9.915	90	7.215
105	7.875	105	5.865
120	5.595	120	4.245
135	3.06	135	2.385
142.5	1.68	142.5	1.35
150	0	150	0

Table (2) The C_{Pu} of W.T. results at V = 36 m/s

Point	1	2	3	4	5	6	7	8	9	10
x/c	0.01	0.02	0.05	0.1	0.175	0.25	0. 5	0.75	0.9	0.95
$a = -9^\circ$	-0.095	- 0.212	- 0.433	- 0.616	- 0.837	- 1.006	- 0.913	- 0.867	- 0.695	- 0.588
$a = -3^\circ$	-0.103	- 0.515	- 1.029	- 1.417	- 1.423	- 1.381	- 1.212	- 0.951	- 0.786	- 0.685
$a = 0^\circ$	-0.243	- 0.749	- 1.254	- 1.628	- 1.501	- 1.423	- 1.325	- 1.102	- 0.864	- 0.812
$a = 6^\circ$	-2.015	- 2.730	- 2.741	- 2.442	- 2.266	- 1.856	- 1.511	- 1.356	- 0.988	- 0.884
$a = 15^\circ$	-2.655	- 3.126	- 3.723	- 3.568	- 3.223	- 2.875	- 1.895	- 1.421	- 1.095	-0.971

Table (3) The C_{PL} of W.T. results at V=36 m/s

Point	1	2	3	4	5	6	7	8	9	10
x/c	0.01	0.02	0.05	0.1	0.175	0.25	0. 5	0.75	0.9	0.95
$a = -9^\circ$	-1.221	-2.312	-3.544	-3.125	-2.899	-2.679	-1.665	-1.431	-0.983	-0.721
$a = -3^\circ$	-0.638	-0.901	-2.487	-1.936	-1.785	-1.689	-1.503	-1.315	-0.942	-0.696
$a = 0^\circ$	-0.241	-0.622	-1.252	-1.281	-1.366	-1.298	-1.247	-0.955	-0.803	-0.518
$a = 6^\circ$	-0.115	-0.156	-0.372	-0.705	-0.851	-0.958	-0.920	-0.898	-0.788	-0.609
$a = 15^\circ$	-0.055	-0.086	-0.111	-0.125	-0.365	-0.467	-0.763	-0.805	-0.711	-0.573

Table (4) C_L, C_D, C_m at V=36 m/s for both Theoretical from Design Foil and Experimental from W.T.

Experimental	$a = 0^\circ$	$a = 6^\circ$	$a = 15^\circ$	$a = -3^\circ$	$a = -9^\circ$
C_L	0.1535418	0.9047896	2.149586	-0.2756887	-0.9491458
C_D	0.0091578	0.0321457	0.0263564	0.0122145	0.0181544
C_m	-0.0245876	-0.0414578	-0.0814587	0.0055478	0.0352634
Theoretical	$a = 0^\circ$	$a = 6^\circ$	$a = 15^\circ$	$a = -3^\circ$	$a = -9^\circ$
C_L	0.1442345	0.8151023	1. 859238	-0.1995871	-0.862580
C_D	0.0074351	0.0121346	0.0165014	0.0088245	0.0155984
C_m	-0.0104507	-0.0335472	-0.076548	-0.0026442	0.0227267

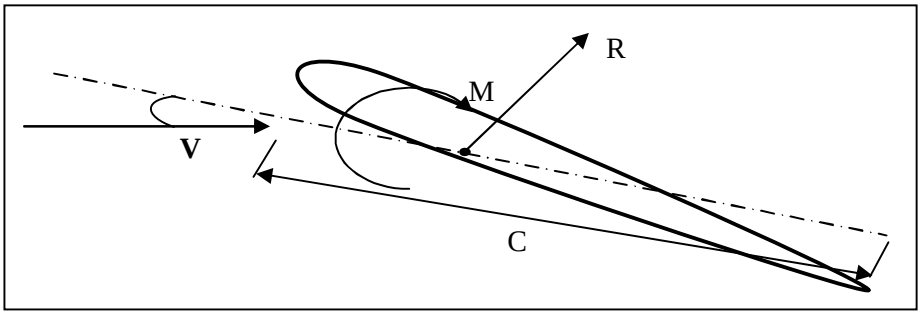

Figure (1) Section of an airfoil at incidence a to the fluid stream, which is assumed to be from left to right at a speed of (v).

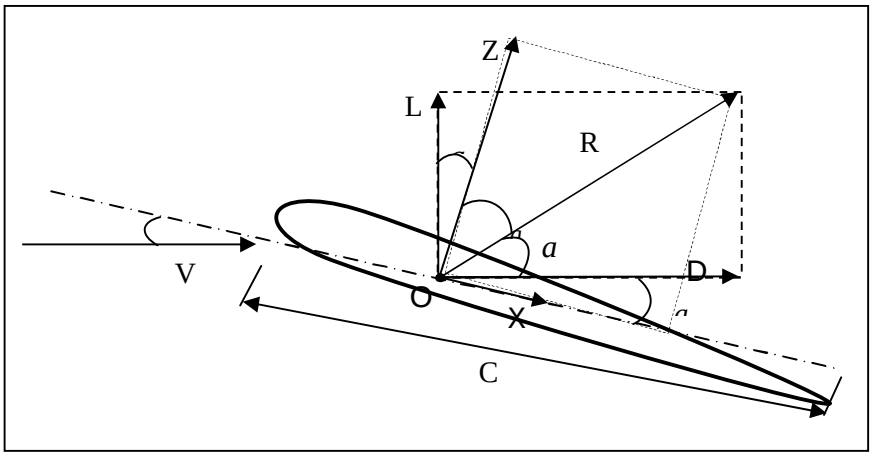

Figure(2) The conversion from one pair to the other may be performed by reference in which C_R, the coefficient of the resultant both of C_x, C_z and of C_L and C_D.

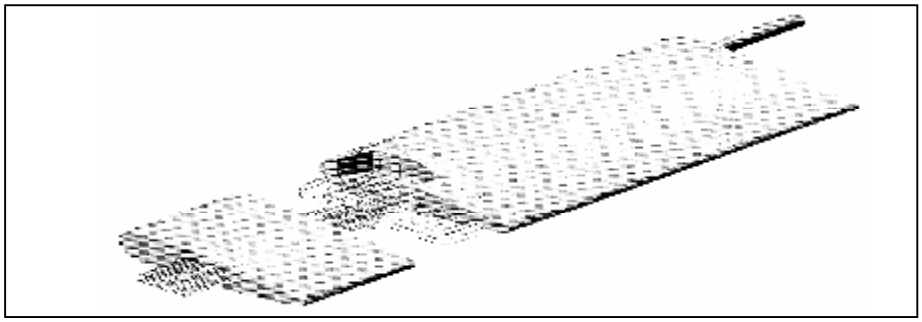

Figure (3) The Model of Section of NACA 23015 showing the pressure tubes inside the wing

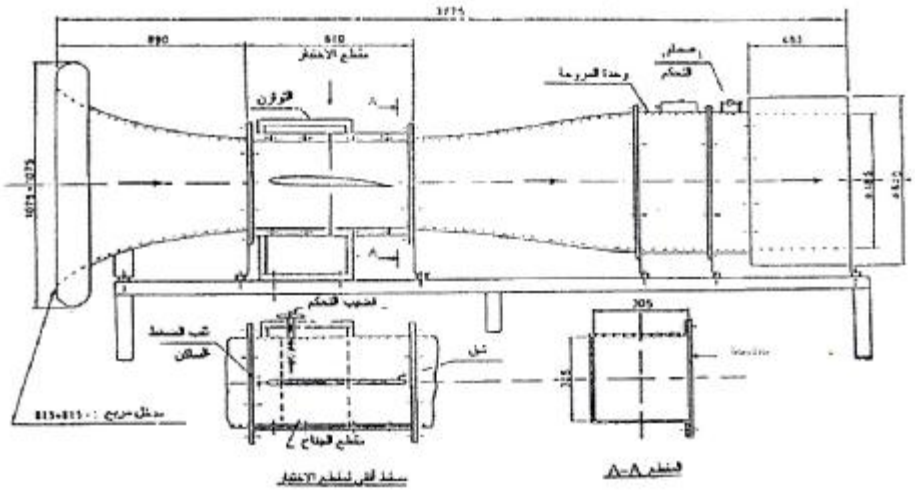

Figure (5) Wind Tunnel Dimension [all dimensions in mm]

Figure (6) Wind Tunnel Device (Open Circuit) Side view

Figure **(7) Working Section of Wind Tunnel and the Model Mounted**

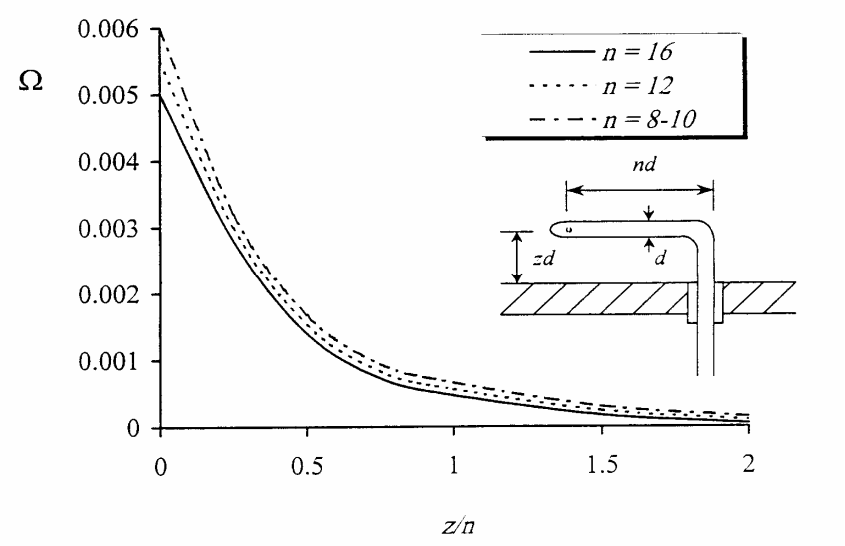

Figure (8) Pitot Static Tube and the correction factor curve

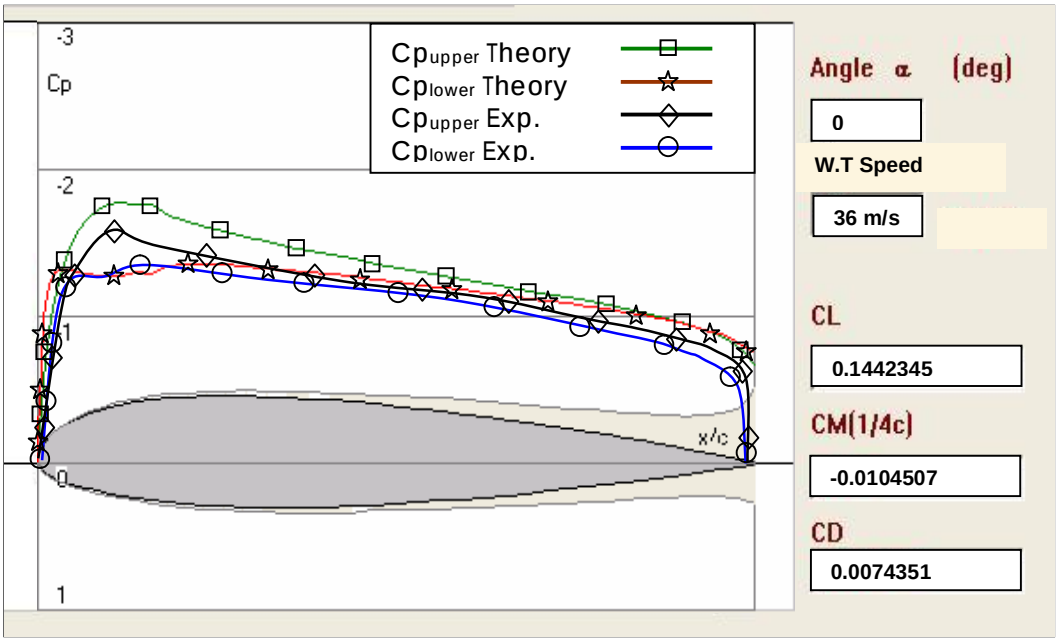

Figure (9) The relationship between the C_{Pu} & C_{PL} ,for both theoretical and experimental and x/c for $\alpha = 0^{o}$, V = 36 m/s from Design Foil Program

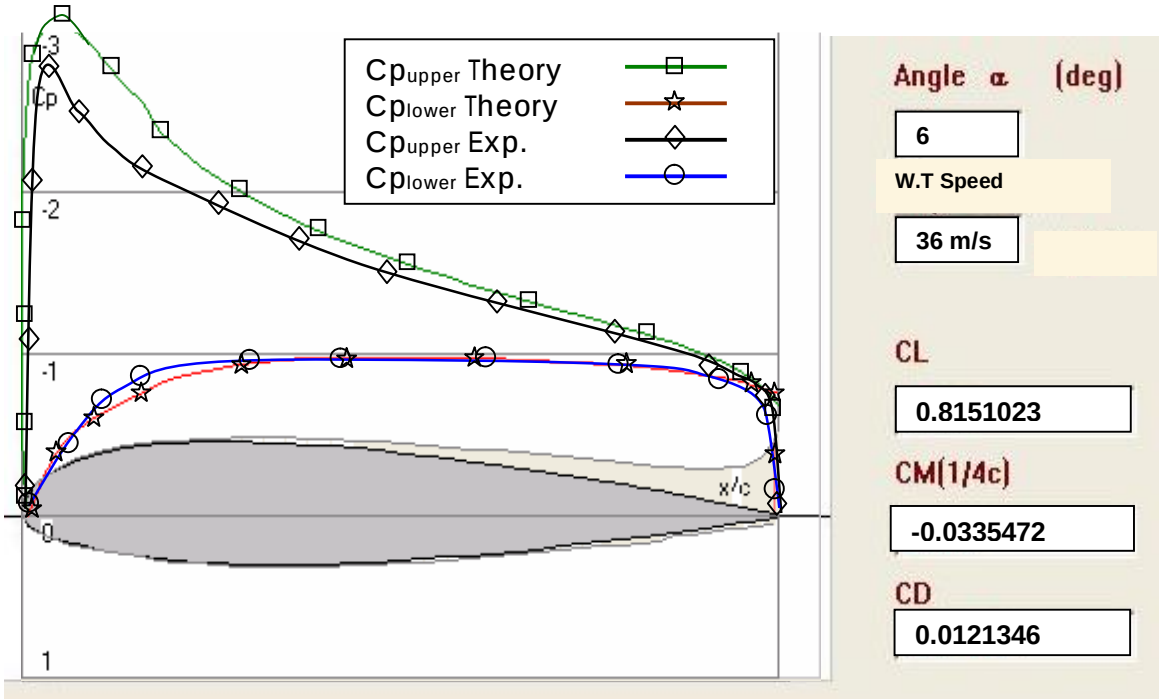

Figure (10) The relationship between the C_{Pu} & C_{PL} ,for both theoretical and experimental and x/c for $\alpha = 6^{o}$, V = 36 m/s from Design Foil Program

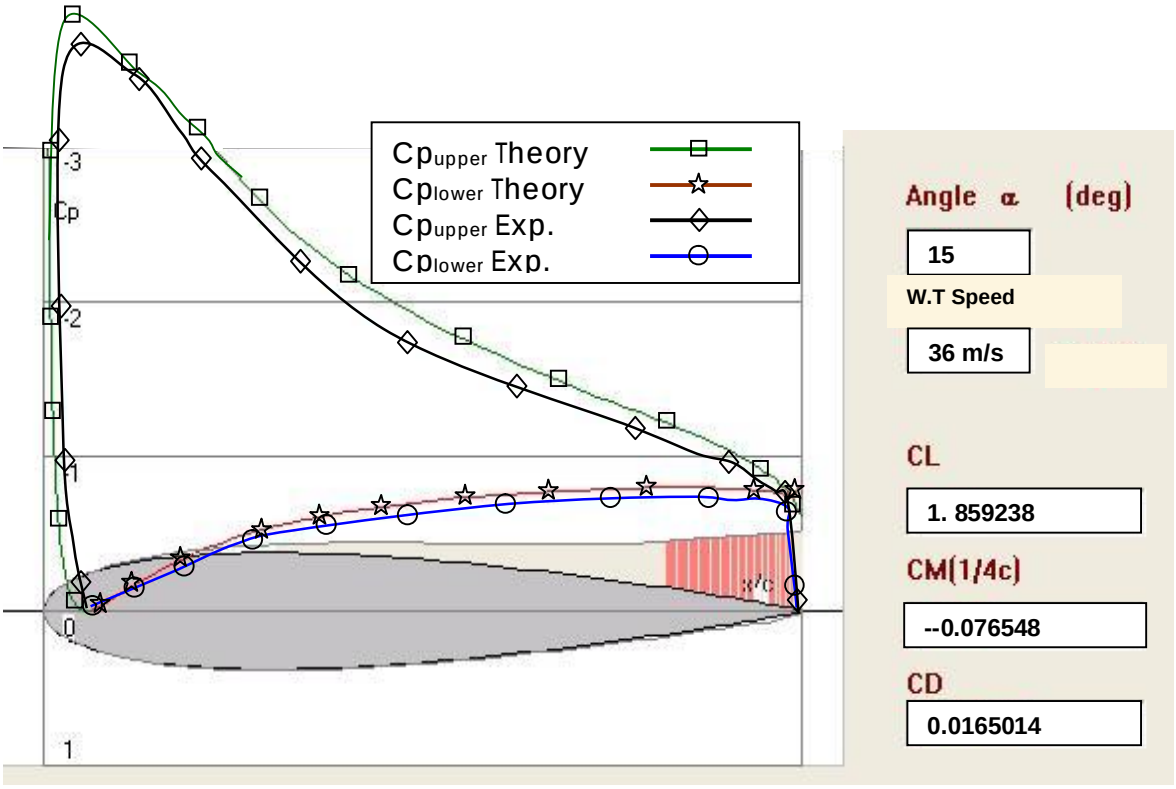

Figure (11) The relationship between the C_{Pu} & C_{PL} ,for both theoretical and experimental and x/c for $\alpha = 15^{o}$, V = 36 m/s from Design Foil Program

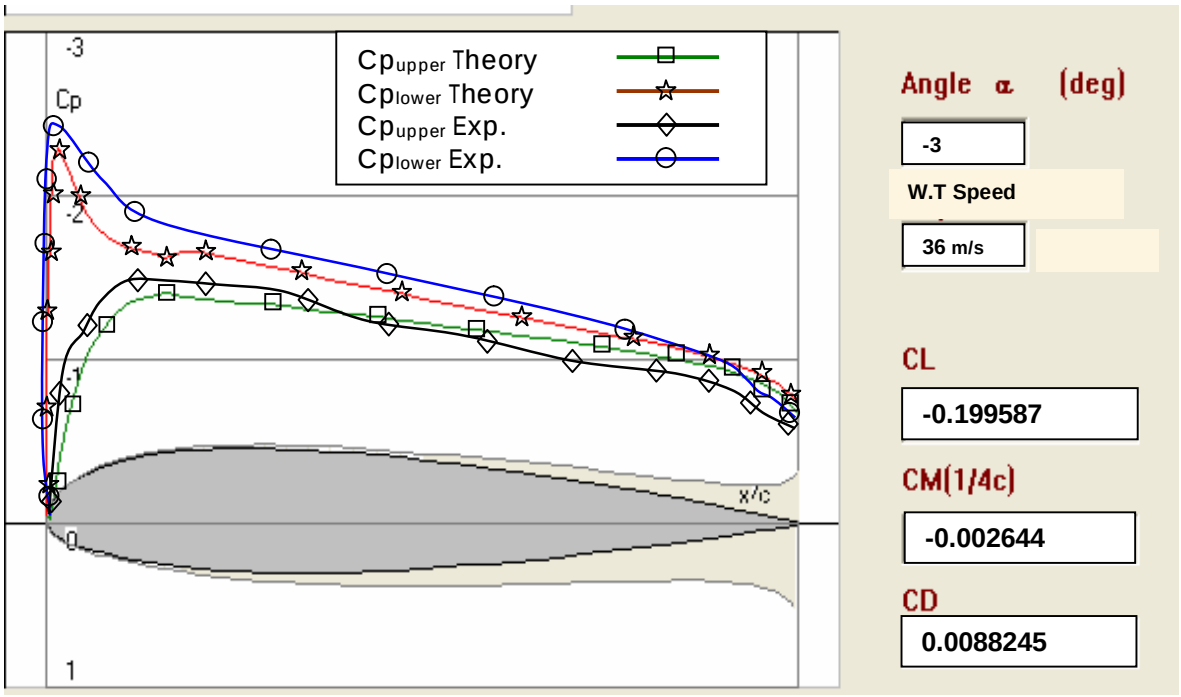

Figure (12) The relationship between the C_{Pu} & C_{PL} ,for both theoretical and experimental and x/c for $\alpha = -3^{o}$, V = 36 m/s from Design Foil Program

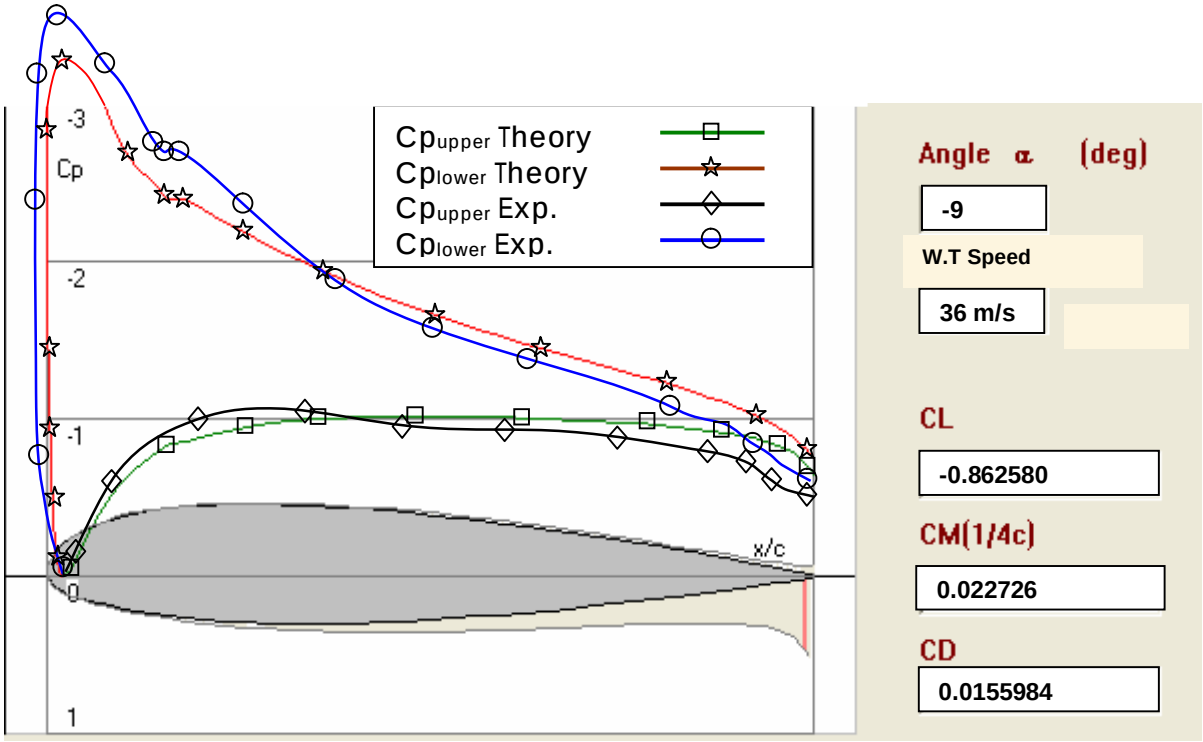

Figure (13) The relationship between the C_{Pu} & C_{PL} ,for both theoretical and experimental and x/c for $\alpha = -9^{0}$, V = 36 m/s from Design Foil Program

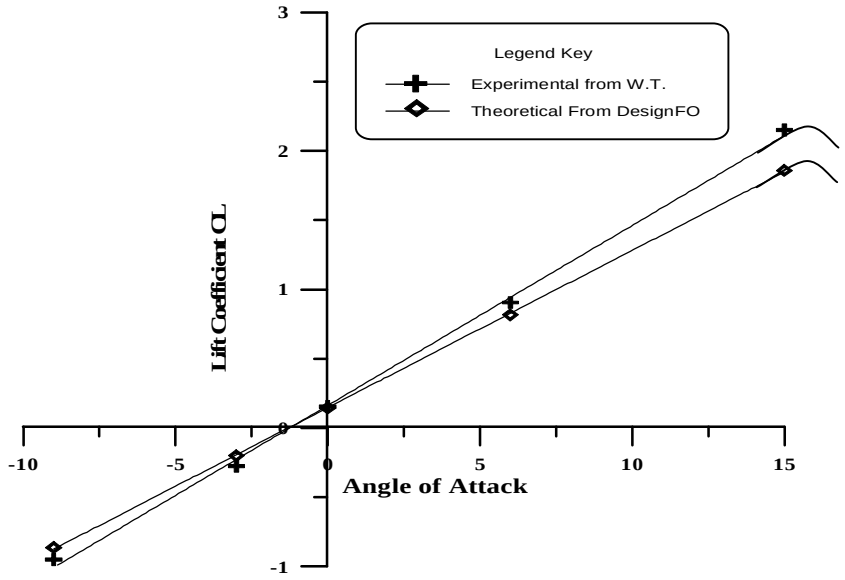

Figure (14) The Lift Coefficient C_L for both Theoretical form Design Foil and Experimental from W.T. at different Angles of attack and Velocity of 36 m/s

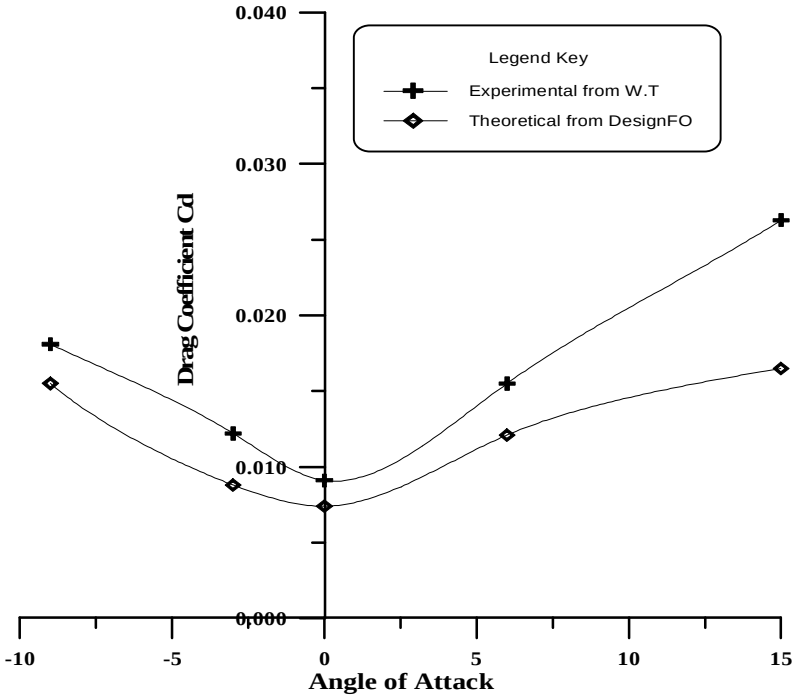

Figure (15) The Drag Coefficient C_d for both Theoretical form Design Foil and Experimental from W.T. at different Angles of attack and Velocity of 36 m/s

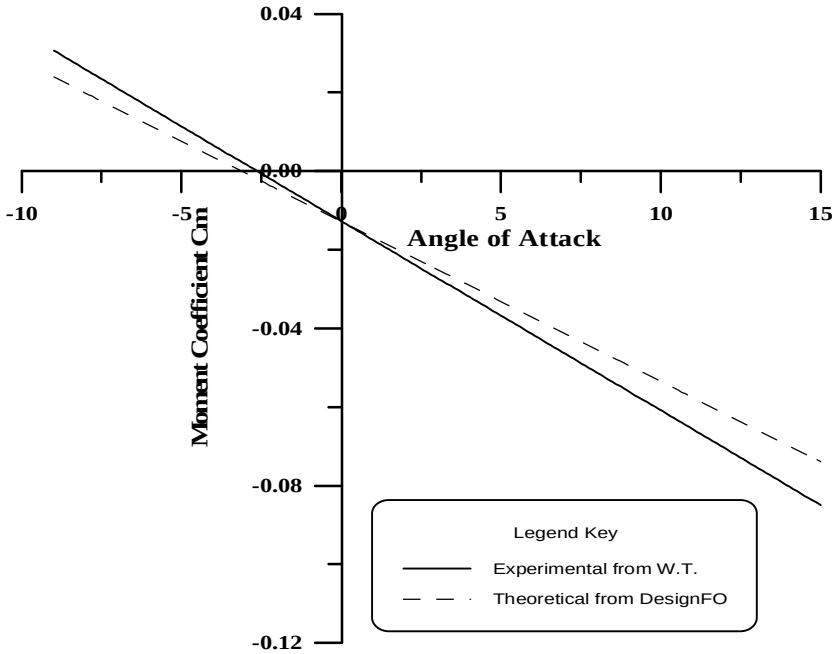

Figure (16) The Moment Coefficient C_d for both Theoretical form Design Foil and Experimental from W.T. at different Angles of attack and Velocity of 36 m/s

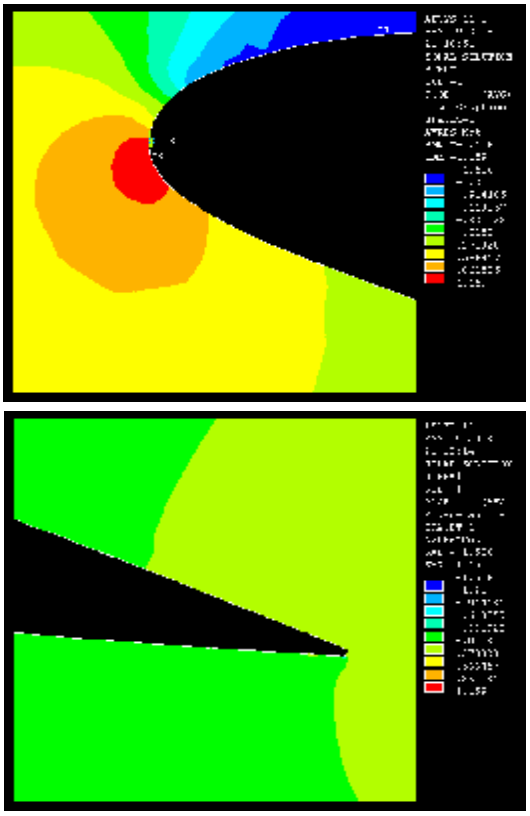

Figure (17) The Pressure Coefficient C_p for both Tip & Tail of the section at Angle of attack = 15^o & Velocity of 36 m/s

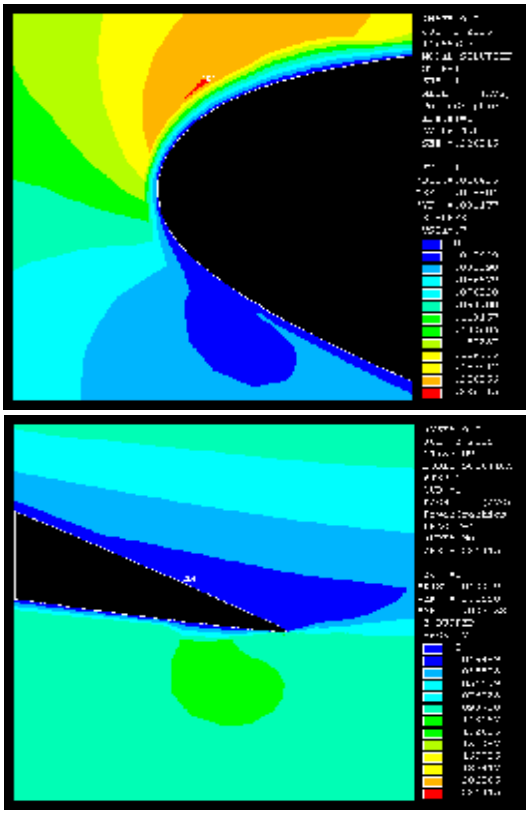

Figure (18) The Mach No. for both Tip & Tail of the section at Angle of attack = 15^o & Velocity of 36 m/s

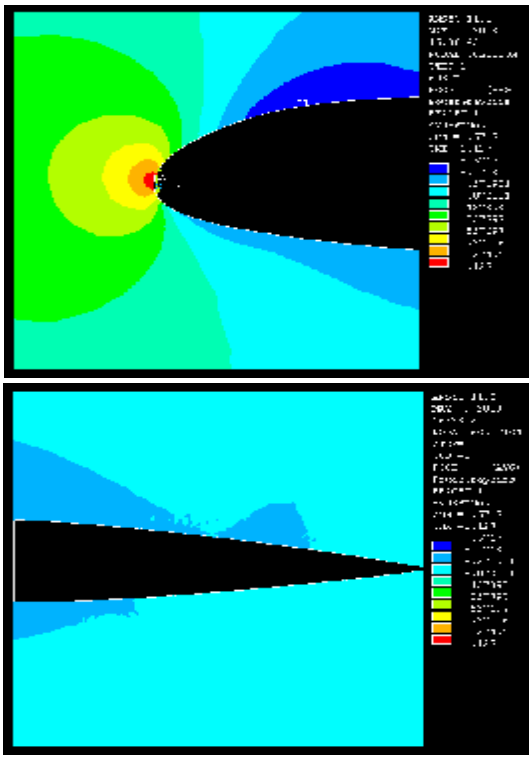

Figure (19) The Pressure Coefficient C_p for both Tip & Tail of the section at Angles of attack = 0^o & Velocity of 36 m/s

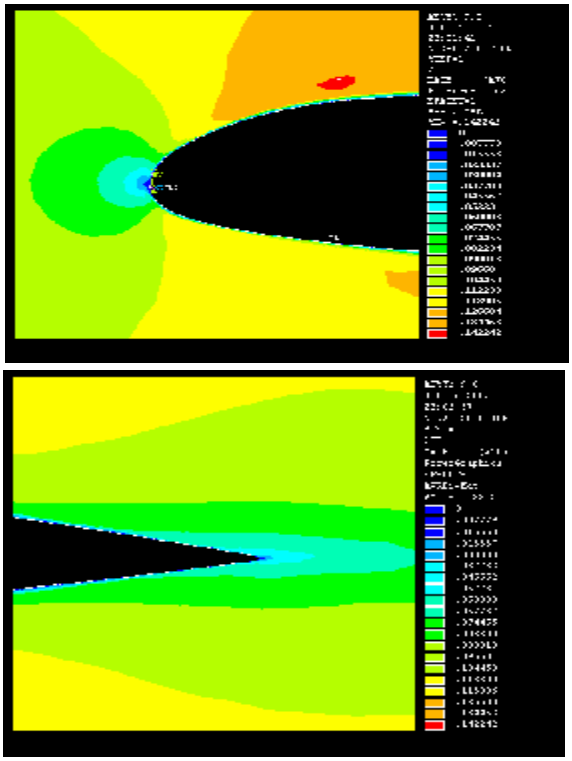

Figure (20) The Mach No. for both Tip & Tail of the section at Angles of attack = 0^o & Velocity of 36 m/

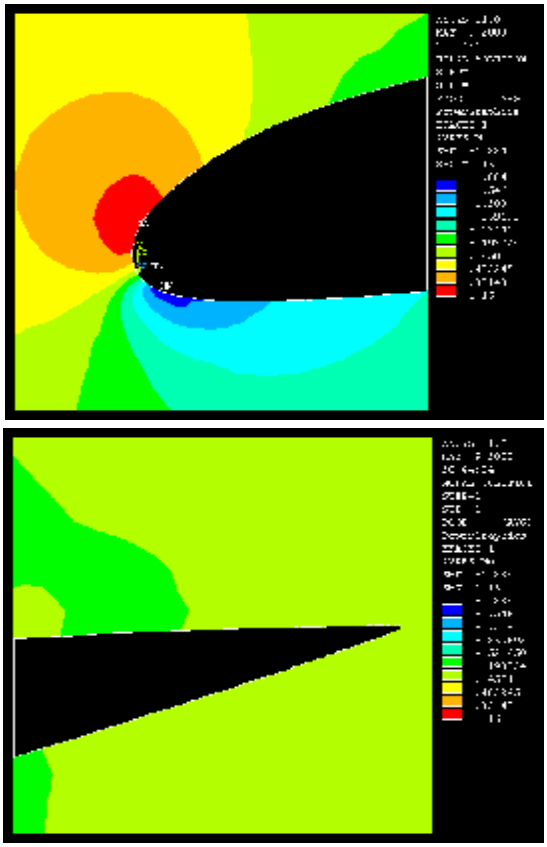

Figure (21) The Pressure Coefficient C_p for both Tip & Tail of the section at Angles of attack = -9° & Velocity of 36 m/s

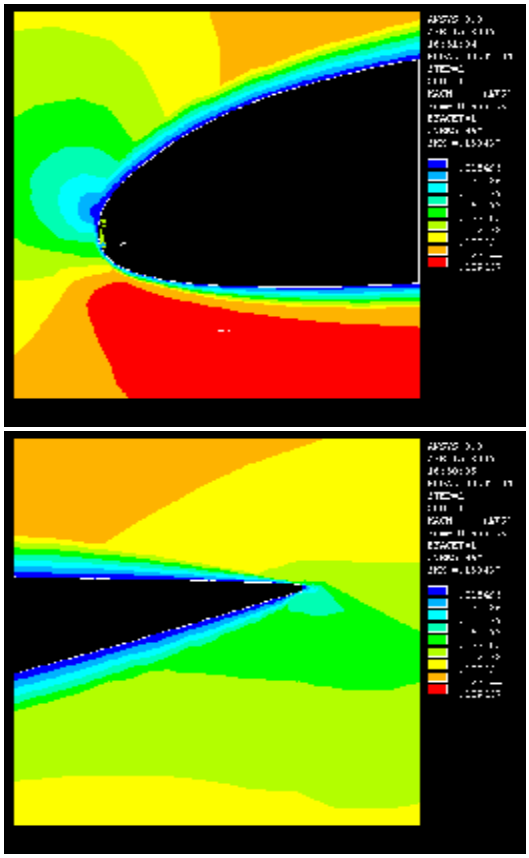

Figure. (22) The Mach No. for both Tip & Tail of the section at angle of attack = -9° & Velocity of 36 m/s